Radionuclide Immobilization in Phases Formed by Corrosion of Spent Nuclear Fuel: The Long-Term Assessment

Rodney C. Ewing

Departments of Nuclear Engineering & Radiological Sciences and Geological Sciences
University of Michigan, Ann Arbor, MI 48109

EMSP # DE-FG07-97ER14816

Photomicrograph of a polished thin section (# 637) showing black uraninite UO_{2+x} and its alteration to yellow schoepite. Jefferson, Colorado, metasedimentary. Field of view 3.5 cm wide

INTRODUCTION

Spent Nuclear Fuel (SNF) is essentially UO_2 with approximately 4-5 atom% actinides and fission products. A number of these nuclides have long half-lives, e.g., ^{239}Pu (2.41×10^4 years); ^{237}Np (2.14×10^6 years); ^{129}I (1.5×10^7 years); ^{79}Se (1.1×10^6 years); and ^{99}Tc (2.13×10^5 years).

World-wide, approximately 130,000 metric tons of heavy metal (MTHM) of SNF had accumulated by 1998. In the USA alone there were 33,700 MTHM in 1996 and the end-of-life projection for current nuclear power plants is approximately 86,000 MTHM. The DOE currently investigates the proposed Yucca Mountain repository for final disposal of the SNF generated in the USA. This repository is located under nominally oxidizing conditions under which UO_2 is unstable.

The long-term behavior of UO_2 is therefore an essential concern in the evaluation of a safe disposal of SNF in the geosphere.

Direct verification of the successful confinement for these long-term periods is impossible, but it can be evaluated through analysis of natural systems. Specifically by physicochemical studies of uraninite and its naturally occurring alteration products.

In this research project we address the following issues:

- ***What are the corrosion products and the thermodynamic properties of uranyl phases that forms during corrosion of SNF under oxidizing conditions?***

- ***Are nuclear reaction products retained in the uranyl phases that forms during oxidative corrosion of SNF/uraninite?***

- ***Is long-term retardation of nuclear reaction products documented from natural systems?***

- ***What is the geochemical behavior of impurities during alteration of uraninite under reducing conditions?***

1. GIBBS FREE ENERGY AND ENTHALPY FOR U^{6+} PHASES: MODEL FOR EMPIRICAL PREDICTIONS

The thermodynamic data base for U^{6+} phases is limited. An effort has been made to estimate the standard Gibbs free energy (ΔG^0_f) and enthalpy (ΔH^0_f) of formation of the U^{6+} phases based on their structural components. The accuracy of this method is 0.08 and 0.10% for ΔG^0_f and ΔH^0_f, respectively. Well below uncertainties for experimental data.

Structural Components for Thermodynamic Estimates

Uranyl phases are decomposed into structural units that are combined with hydrogen bonds or low-valence cations. Examples are shown in Table 1.1.

Table 1.1: Constituent structural components of uranyl minerals.

schoepite	$[(UO_2)_8O_2(OH_{12}].12H_2O$	$6H_2O_{(s)}+8Ur\Phi_5+12H_2O_{(H)}$
becquelerite	$Ca[(UO_2)_3O_2(OH_3]_2.8H_2O$	$CaO_{(I)}+3H_2O_{(s)}+6Ur\Phi_5+8H_2O_{(H)}$
protasite	$Ba[(UO_2)_3(OH)_2].3H_2O$	$BaO_{(I)}+H_2O_{(s)}+3Ur\Phi_5+3H_2O_{(H)}$
curite	$Pb_3[(UO_2)_8O_8(OH_6].3H_2O$	$3PbO_{(I)}+3H_2O_{(s)}+6Ur\Phi_5+2Ur\Phi_4+3H_2O_{(H)}$
boltwoodite	$(K,Na)[(UO_2)(SiO_3OH)].1.5H_2O$	$0.5(K,Na)_2O_{(I)}+0.5H_2O_{(s)}+Ur\Phi_5+SiO_{2(IV)}+1.5H_2O_{(H)}$
chernikovite	$[(UO_2)H(PO_4)].4H_2O$	$0.5H_2O_{(s)}+Ur\Phi_4+0.5P_2O_{5(IV)}+4H_2O_{(H)}$

Uranium: U^{6+} forms the sub-linear uranyl ion, UO_2^{2+}, that can be coordinated by 4, 5, and 6 oxygens: $Ur\Phi_4$; $Ur\Phi_5$; and $Ur\Phi_6$. The thermodynamic data for these structural components appear to be similar, but significant differences are expected due to structural distortions.

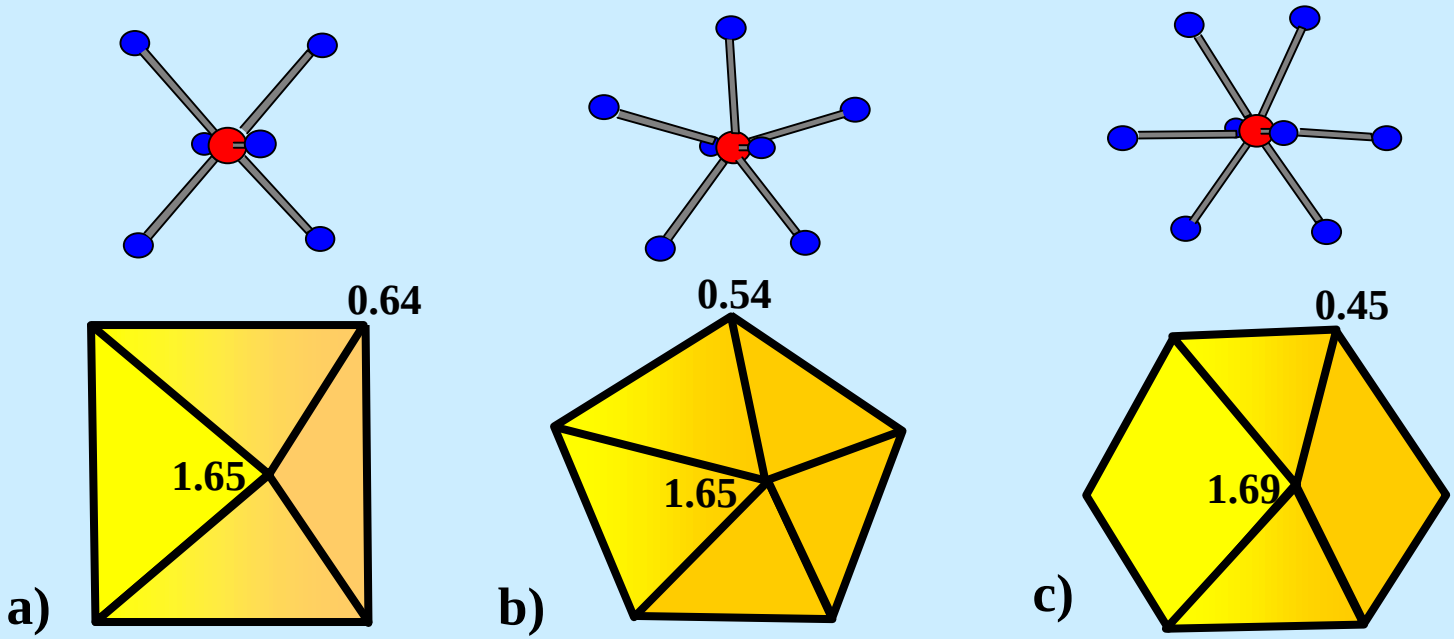

Fig. 1.1: Illustration of the uranyl structures a) $Ur\Phi_4$; b) $Ur\Phi_5$; and c) $Ur\Phi_6$.

High Valence Cations: The thermodynamic values of the high valence cations are calculated for fictive oxide compounds:

$SiO_{2(IV)}$, $SO_{3(IV)}$, $CO_{2(III)}$, $N_2O_{5(III)}$, $P_2O_{5(IV)}$

H_2O: Water can be present as structural and hydration water and are treated as two different species:

Structural Water, OH^-: $H_2O_{(S)}$
Hydration Water, H_2O: $H_2O_{(H)}$

Low-Valence Cations: The interconnecting low-valence cations are calculated as fictive oxide compounds:

$Na_2O_{(I)}$, $MgO_{(I)}$, $CaO_{(I)}$, $BaO_{(I)}$, $Li_2O_{(I)}$, $K_2O_{(I)}$, $Rb_2O_{(I)}$, $Cs_2O_{(I)}$

Thermodynamic Calculations and New Data

Regression analysis of thermodynamic data from 99 known phases enabled determination of g_i and h_i for each of the structural components. Hence, letting n_i be the number of moles of component *i* in the uranyl phase, the ΔG^0_f and ΔH^0_f are estimated by the following relations:

$$\Delta G^0_f = \Sigma n_i g_i$$
$$\Delta H^0_f = \Sigma n_i h_i$$

The resulting thermodynamic data for a number of uranyl phases are listed in Table 1.2 ($\Delta G^0_{f,298}$) and Table 1.3 ($\Delta H^0_{f,298}$), respectively.

Table 1.2: Measured and predicted $\Delta G^{0}_{f,298}$ values for uranyl phases and the related residuals. Phases marked with * were included among the 99 phases that formed the data base.

Formula	Measured $G^{f}_{0,298}$ (KJ/mol)	Predicted $G^{f}_{0,298}$ (KJ/mol)	Residuals (KJ/mol)	Percent residual
*$[(UO_2)_8O_2(OH_{12}].10H_2O$	-13092.0 ± 6.8	-13127.1	35.1	0.27
*β-$UO_2(OH)_2$	-1398.0 ± 1.8	-1399.0	0.3	0.02
*$UO_3.0.9H_2O$	-1374.6 ± 2.5	-1375.2	0.6	0.04
*$(UO_2)(SO_4).3H_2O$	-2416.6 ± 1.8	-2416.9	0.3	0.01
*$Na[(UO_2)(SiO_3OH)].1.5H_2O$	-2844.8 ± 3.9	-2838.9	-5.9	0.21
*$[(UO_2)H(PO_4)].4H_2O$	-3064.7 ± 2.4	-3063.5	-1.2	0.04
$(UO_2)_3(PO_4)_2$	-5116.0 ± 5.5	-5132.2	16.2	0.32
$(UO_2)_3(PO_4)_2.4H_2O$	--6139.0 ± 6.4	-6093.4	-45.6	0.74
$Mg_2(UO_2)(CO_3)_3.18H_2O$	-7881.1 ± 8.0	-7862.9	-18.2	0.23
$Na_2Ca(UO_2)(CO_3)_3.6H2O$	-5207.1 ± 24.0	-5215.7	8.64	0.17

Table 1.3: Measured and predicted $\Delta H^0_{f,298}$ values for uranyl phases and the related residuals. Phases marked with * were included among the 99 phases that formed the data base.

Formula	Measured $H^f_{0,298}$ (KJ/mol)	Predicted $H^f_{0,298}$ (KJ/mol)	Residuals (KJ/mol)	Percent residual
*$[(UO_2)_8O_2(OH_{12}].10H_2O$	-14608.8 ± 13.6	-14625.4	16.6	0.11
*β-$UO_2(OH)_2$	-1533.8 ± 1.3	-1533.7	-0.1	0.01
*$UO_3.0.9H_2O$	-1506 ± 1.3	-1503.7	-2.6	0.17
*$(UO_2)(SO_4).3H_2O$	-2751.5 ± 4.6	-2753.4	1.9	0.07
*$Na[(UO_2)(SiO_3OH)].1.5H_2O$	---	---	---	---
*$[(UO_2)H(PO_4)].4H_2O$	-3470.0 ± 7.8	-3467.2	-2.8	0.08
$(UO_2)_3(PO_4)_2$	-5491 ± 3.5	-5512.3	21.0	0.38
$(UO_2)_3(PO_4)_2.4H_2O$	--6739 ± 9.1	-6690.9	-48.2	0.74
$Mg_2(UO_2)(CO_3)_3.18H_2O$	-9164.2 ± 20	-9165.7	-1.5	0.02
$Na_2Ca(UO_2)(CO_3)_3.6H2O$	-5893.0 ± 36	-5826.3	-53.1	1.13

2. GEOCHEMICAL AND CRYSTALLO-CHEMICAL RETARDATION OF ^{79}Se AND ^{99}Tc

^{79}Se ($T_{½}$ = 1.1 ×10^6 years) and ^{99}Tc ($T_{½}$ = 2.13 ×10^5 years) are long-lived fissiogenic radionuclides that are chemically and radiologically toxic. Under oxidizing conditions, both radionuclides appear to be highly mobile in the geosphere. Their speciation in oxidized waters and their retardation in U^{6+} phases that form during corrosion of SNF have been analyzed.

Aqueous Speciation

In oxygenated aqueous solutions, selenite (SeO_3^{2-} or $HSeO_3^-$) and selenate (SeO_4^{2-}) are the dominant species of Se; whereas, Tc will mainly occur as TcO_4^- with log $TcO_4^-/TcO(OH)_2^0$ > 2.15 at pH = 4 - 10 (Fig. 2.1).

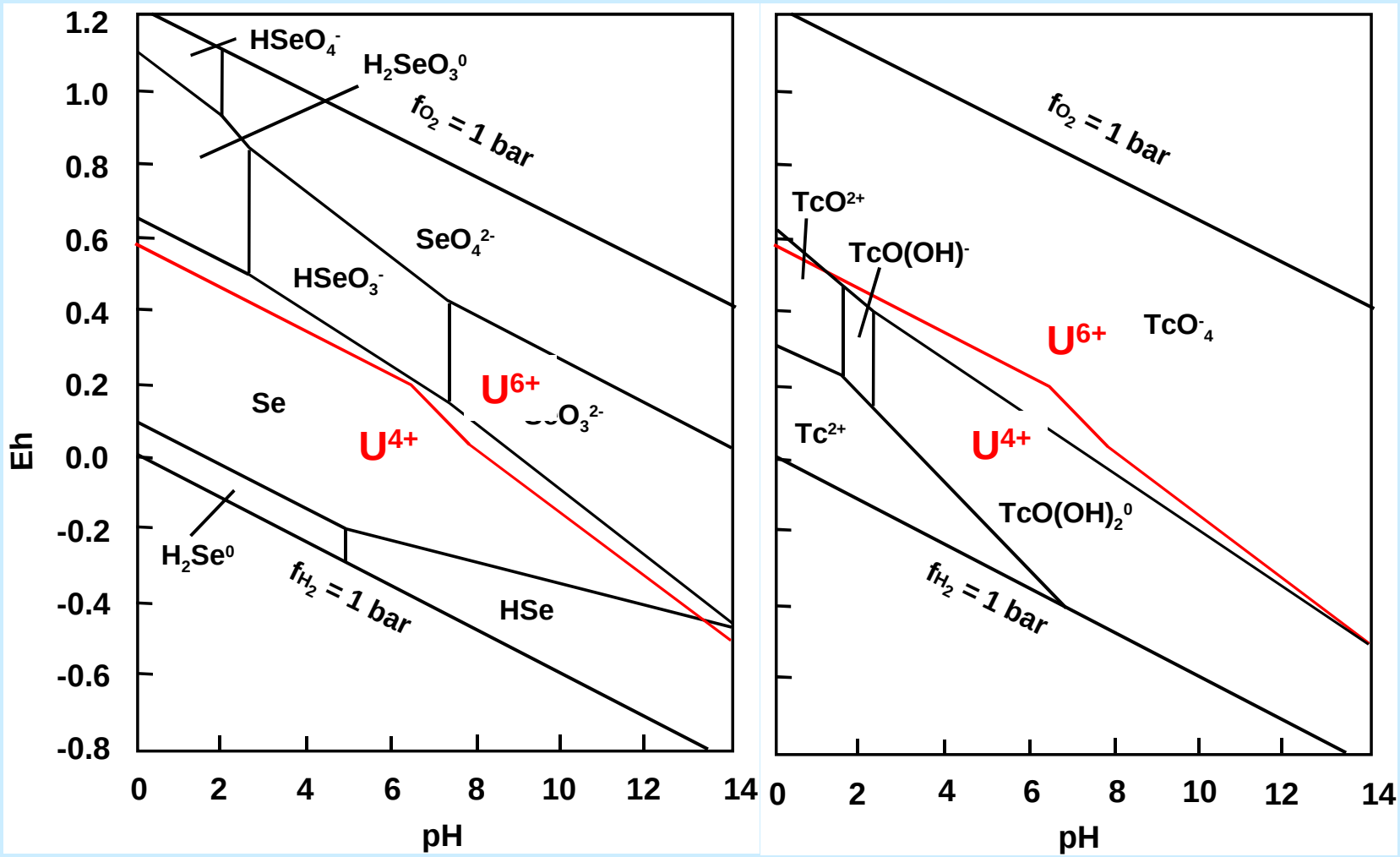

Fig. 2.1: Calculated Eh-pH diagrams for Se and Tc in H_2O. The stability fields for U^{4+} and U^{6+} are marked by the red lines.

Mineralogical Retardation

In nature, Tc occurs in extremely low concentrations and has not been detected in uranyl phases. Theoretical considerations does neither suggest incorporation of Tc due to underbonding of the TcO_4^- component in the uranyl structure.

Six uranyl selenite (SeO_3^{2-} or $HSeO_3^-$) minerals have been described, but no uranyl minerals are known to contain selenate (SeO_4^{2-}). However, the crystal structure of the selenite minerals have only been determined for demaeskerite, derriksite, and guilleminite (Fig. 2.2).

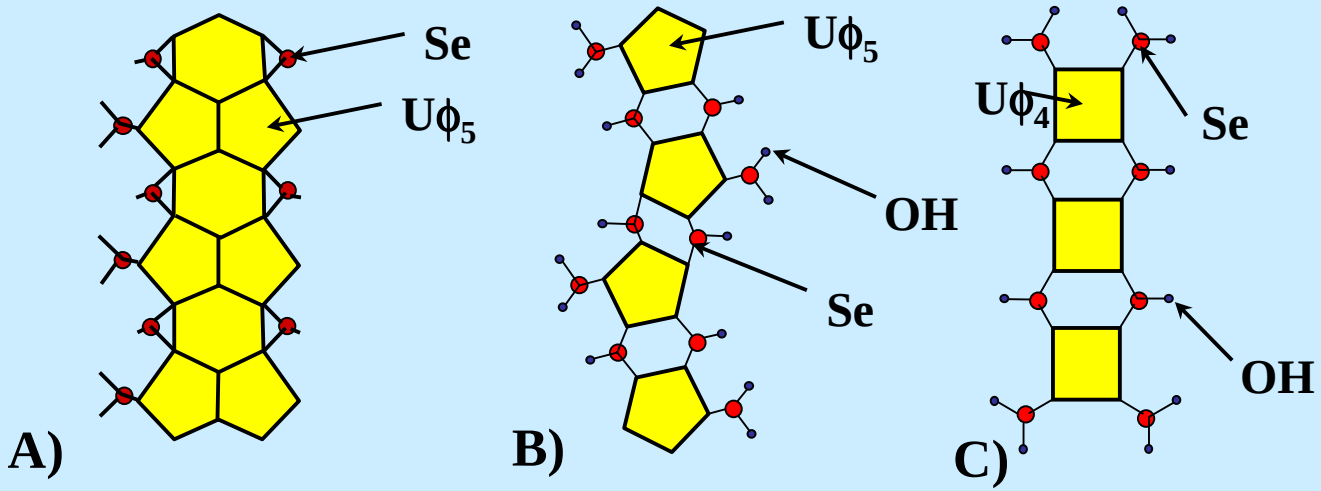

Fig. 2.2: The structural chains that occur in uranyl selenites: A) guilleminite, B) demesmaekerite, and C) derriksite.

In the expected SNF corrosion products, theoretical considerations have shown that selenite is the only ion species that can be incorporated. However, verification is required through experiments. Fig. 2.3 and Table 2.1 illustrates the sites and mechanisms expected in the selenite substitutions in the uranyl phases found to be most important during oxidative corrosion of SNF.

Table 2.1: Summary of the possible substitutions of (SiO_3OH), (SiO_4), and (PO_4) by SeO_3 in selected uranyl phases. [a]Chemical species connected to the apical anion that will be eliminated due to substitution. [b]The bond-valence between the apical anion that will be eliminated due to substitution and the chemical species.

Group	Mineral	Formula	Eliminated species[a]	Bond-valence[b]	Substitution
$SiO_3OH \leftrightarrow SeO_3$	α-uranophane	$Ca[(UO_2)(SiO_3OH)]_2.5H_2O$	H_2O	H-bond	likely
			Ca	0.29	probable
	sklodowskite	$Mg[(UO_2)(SiO_3OH)]_2.6H_2O$	Mg	0.31	probable
	boltwoodite	$(K,Na)[(UO_2)(SiO_3OH)].1.5H_2O$	H_2O	H-bond	likely
			K	0.048	likely
$SiO_4 \leftrightarrow SeO_3$	soddyite	$(UO_2)2(SiO_4).2H_2O$	$Ur\Phi_5$	0.56	unlikely
$PO_4 \leftrightarrow SeO_3$	phurcalite	$Ca_2[(UO_2)_3(PO_4)_2O_2].7H_2O$	Ca	0.33	probable
			Ca	0.46	unlikely
	phosphuranylite	$KCa_2(H_3O)_3(UO_2)[(UO_2)_3(PO_4)_2O_2].8H_2O$	$Ur\Phi_4$	0.67	unlikely

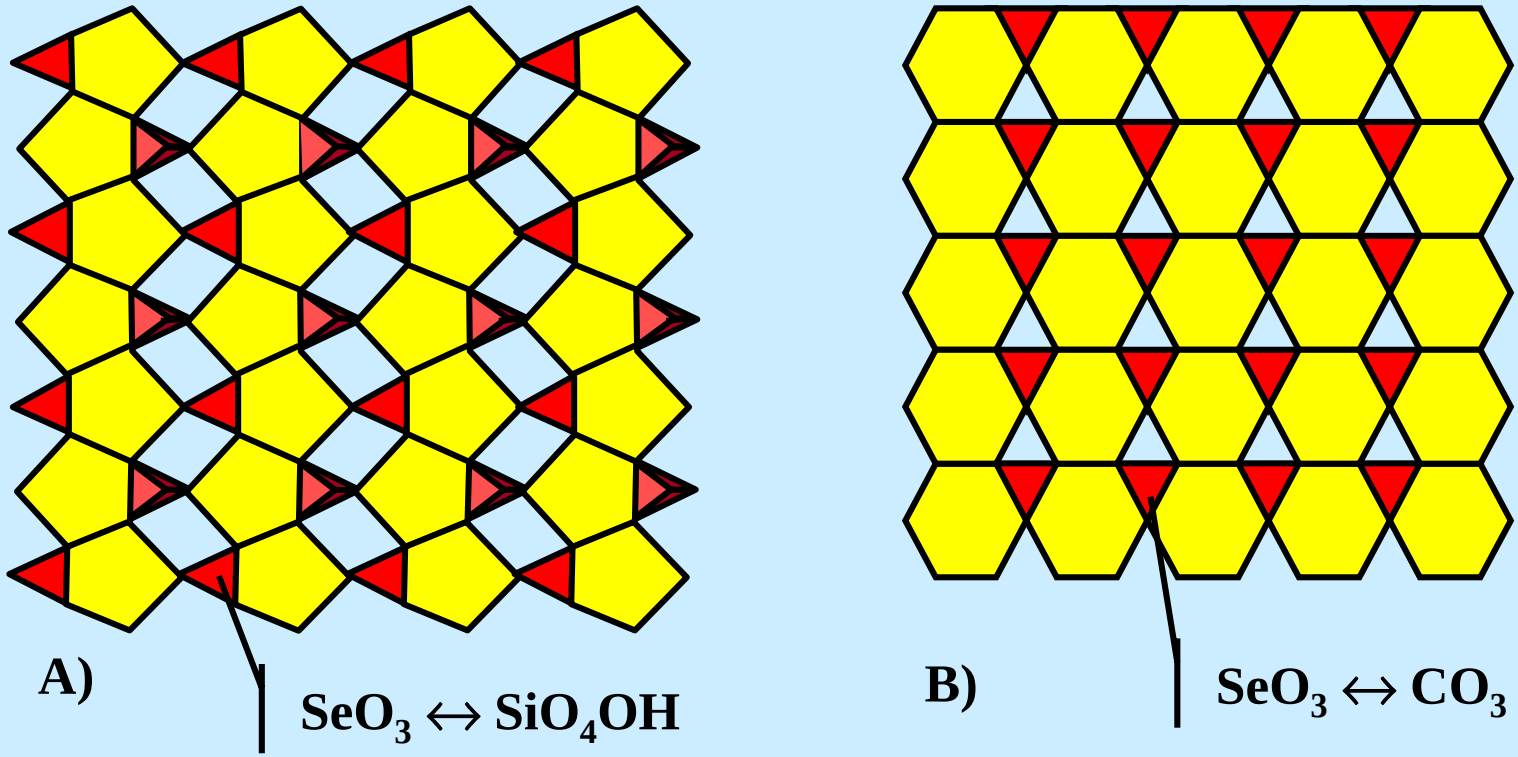

Fig. 2.3: A) Sheets of uranyl α-uranophane anion topology B) Sheets of the rutherfordine anion topology. The sites for substitution with selenite are indicated.

3. ALTERATION PRODUCTS OF URANINITE FROM THE COLORADO PLATEAU

Young uraninite and associated alteration products at the Colorado Plateau were studied in order to determine the fate of trace elements, such as Pb, Ca, Si, Th, Zr, and REE during oxidative corrosion.

Mineralogy

Two types of uraninite were observed: one has high U^{6+} content from 0.587 to 0.808 apfu, close to the stoichiometry of U_3O_8; whereas, the other had a low U^{6+} content (0.212 to 0.489 apfu). Besides uraninite, coffinite, schoepite (Fig. 3.1), calciouranoite, uranophane, fourmarierite, and a Fe-rich uranyl phase were observed. The presence of a Ca-rich calciouranoite in a limestone sample, suggests that the host-rock at some point reacted with the uranium mineralization. The schoepite was usually intimately associated with the high U^{6+} uraninite suggesting its relation to uraninite as an *in situ* corrosion product (Fig. 3.2).

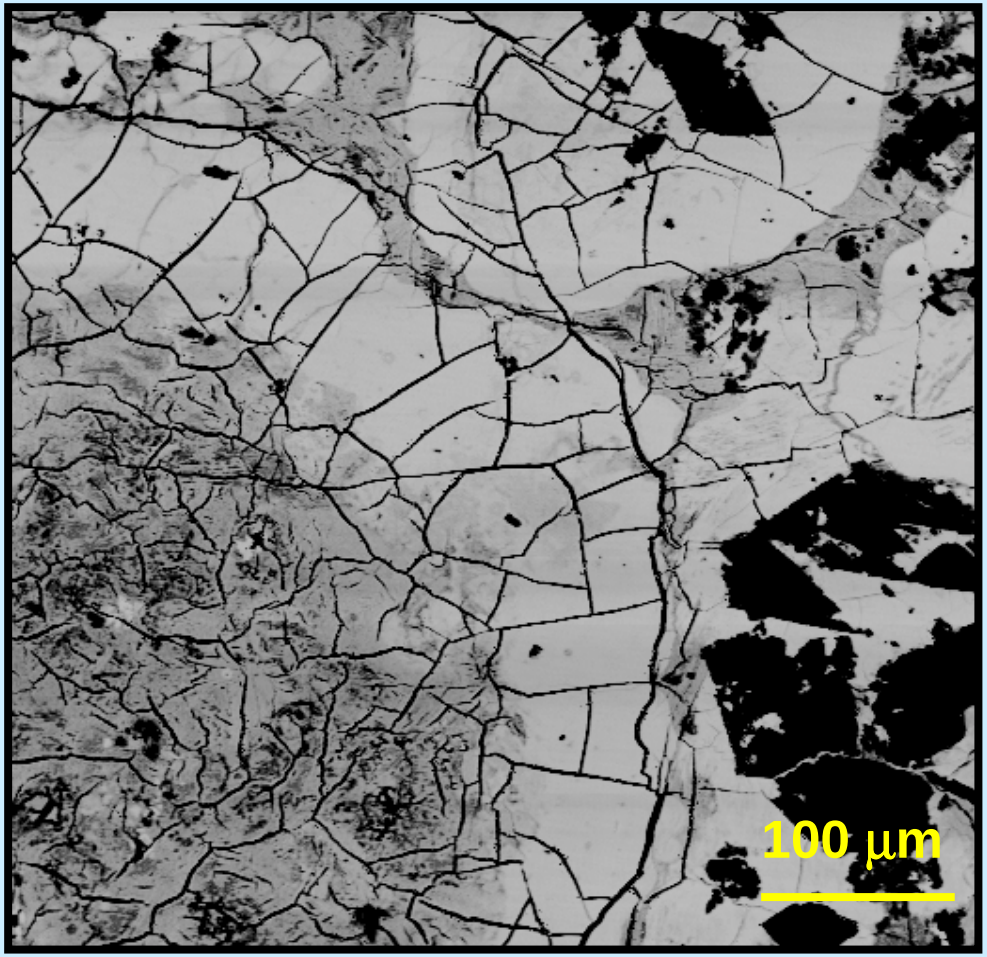

Fig. 3.1: Strongly dehydrated (bright) and weakly dehydrated (grey inner part) schoepite in metasedimentary host rock (Jefferson, CO). The concentric structure and micro-fractures are patterns that may develop during corrosion of spent nuclear fuel.

Fig. 3.2: Concentric structure of uraninite and schoepite in a limestone host rock. A thin schoepite rim (about 10 酸) occurs between the uraninite core (uraninite 1) and over-growths of a late stage uraninite (uraninite 2). (BSEI, Marshall Pass, Saguache, CO)

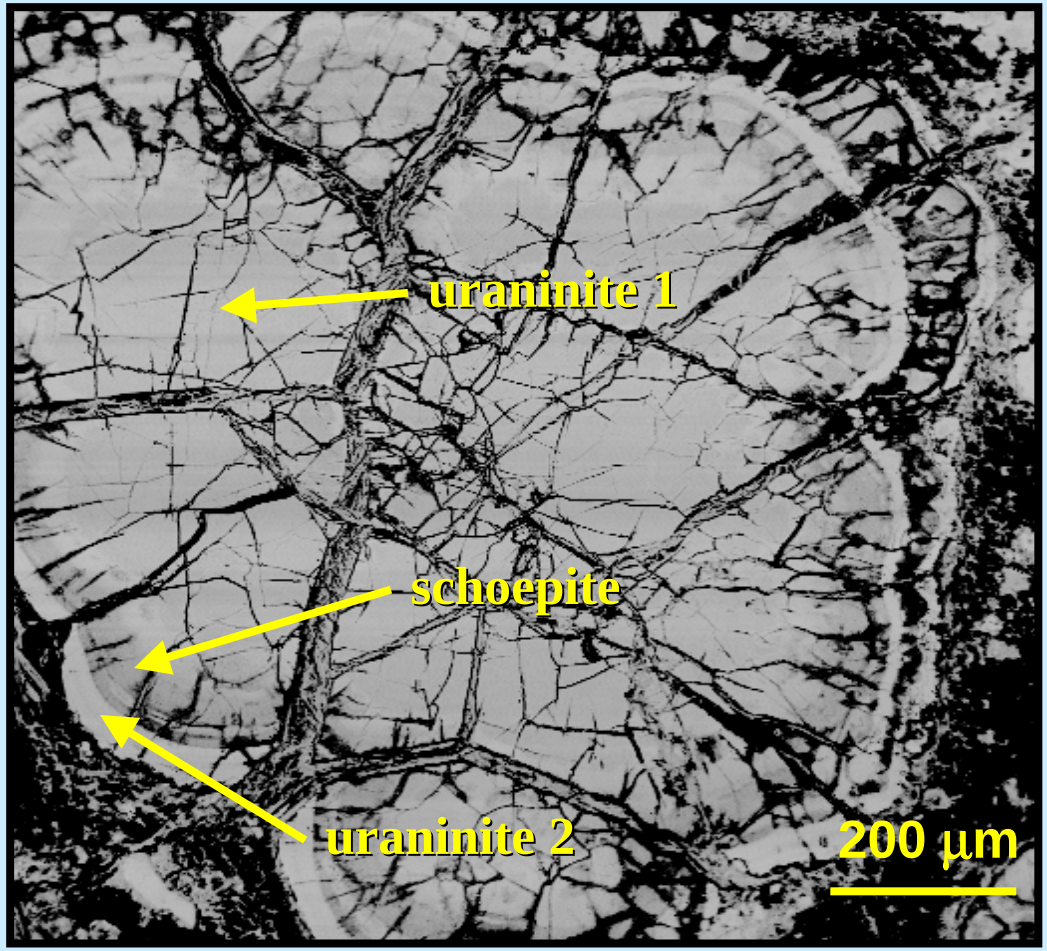

Table 3.1: Compositions of the coexisting uraninite and schoepite (see Fig. 3.2 for uraninite 1 and schoepite)

Phase	uraninite 1	schoepite
UO_3	94.26	87.23
TiO_2	0.29	0.42
ZrO_2	0.37	2.00
PbO	2.51	2.59
FeO	0.24	0.16
CaO	1.41	1.37
Al_2O_3	0.13	0.26
P_2O_5	0.10	0.13
Y_2O_3	0.11	0.15
Ce_2O_3	0.10	0.15
Nd_2O_3	0.14	0.18
Sm_2O_3	0.12	0.14
Eu_2O_3	0.01	0.11
Gd_2O_3	0.08	0.08
Total	99.86	94.99

Conclusion

The oxidative alteration causes loss of U, Pb, and Zr, as compared with their concentration in the uraninite; whereas, several trace elements (Y, Ce, Nd, Sm, Eu, Ti, and Zr) appear to preferentially retarded (Table 3.1). Using the chemical analogy for REE, the results suggests that the release of tri- and tetra-valent transuranium actinides can be retarded by uranyl phases during corrosion of uraninite and spent nuclear fuel.

4. RETARDATION OF NUCLEAR REACTION PRODUCTS IN THE OK¶ OBONDO NATURAL FISSION REACTOR

The Ok□obondo natural fission reactor (RZOKE) occurs at ~ 320 m depth in the Oklo-Ok□obondo uranium mine, SE-Gabon. RZOKE is approximately 2.7 m wide and consists of a 0.5 m thick uraninite-rich (≤ 90 vol.%) reactor core overlain by a ~ 0.5 m thick hydrothermal alteration halo, dominated by Al-chlorite (Fig. 4.1).

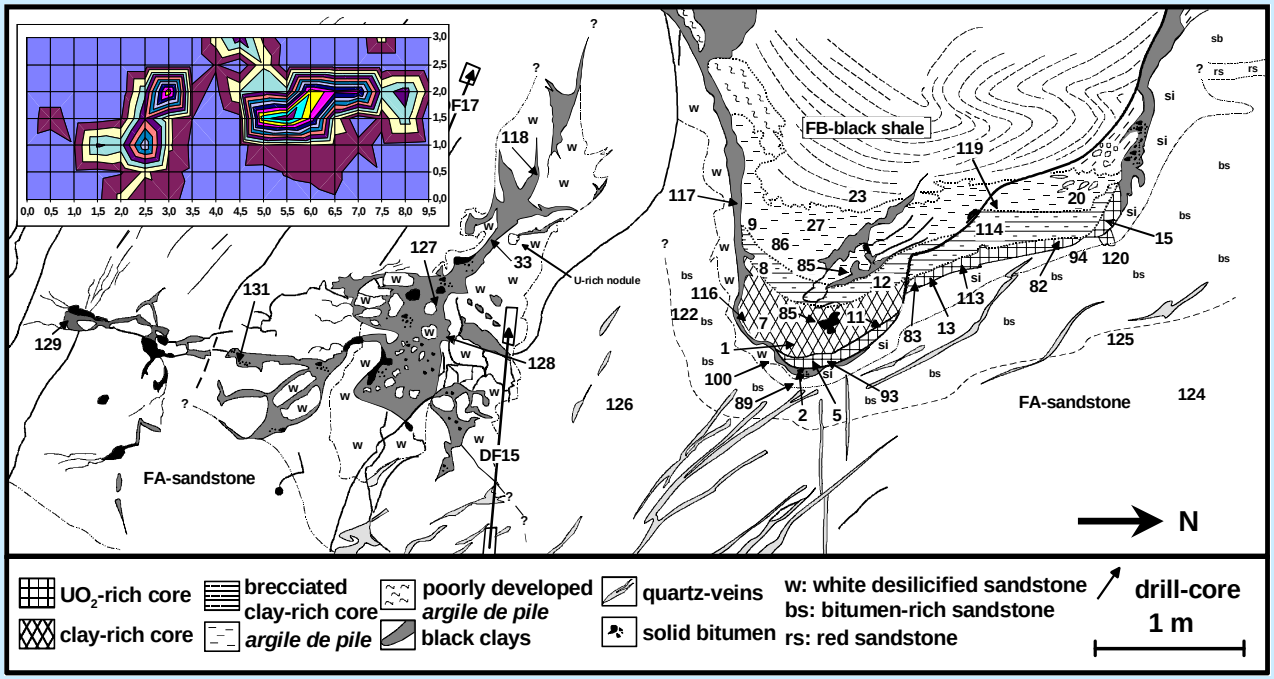

Fig. 4.1: Cross-section of the Ok□obondonatural fission reactor. Numbers refer to the location of samples analyzed in this study. The insert shows the result of a radiometric survey of the tunnel wall.

Phases with Actinides, and Sr, Zr,and REE Fission Products

Uraninite is the primary source term and generally has only been subjected to a minor degree of coffinitization (Fig. 4.2). Electron microprobe analyses of uraninite showed compositional variations in trace element concentrations with location in the reactor zone suggesting a good retention of fissiogenic ^{232}Th (daughter of ^{236}U and ^{240}Pu), ^{90}Zr (daughter of ^{90}Sr), and REE (Ce and Nd) (Fig. 4.3). During local remobilization, these nuclides were incorporated into an accessory U-Zr-silicate (Fig. 4.4). Fissiogenic REE may also have been retained by monazite ($CePO_4$).

Table 4.1: Average composition of uraninite from the reactor zone based on 175 analyses.

UO_2	89.82	±1.59
ThO_2	0.05	±0.04
SiO_2	0.62	±0.14
TiO_2	0.14	±0.16
ZrO_2	0.06	±0.06
PbO	6.48	±0.70
FeO	0.47	±0.07
CaO	1.46	±0.10
Al_2O_3	0.10	±0.20
P_2O_5	0.09	±0.04
SO_3	0.14	±0.11
Ce_2O_3	0.06	±0.03
Nd_2O_3	0.05	±0.05
Total	99.53	±1.58

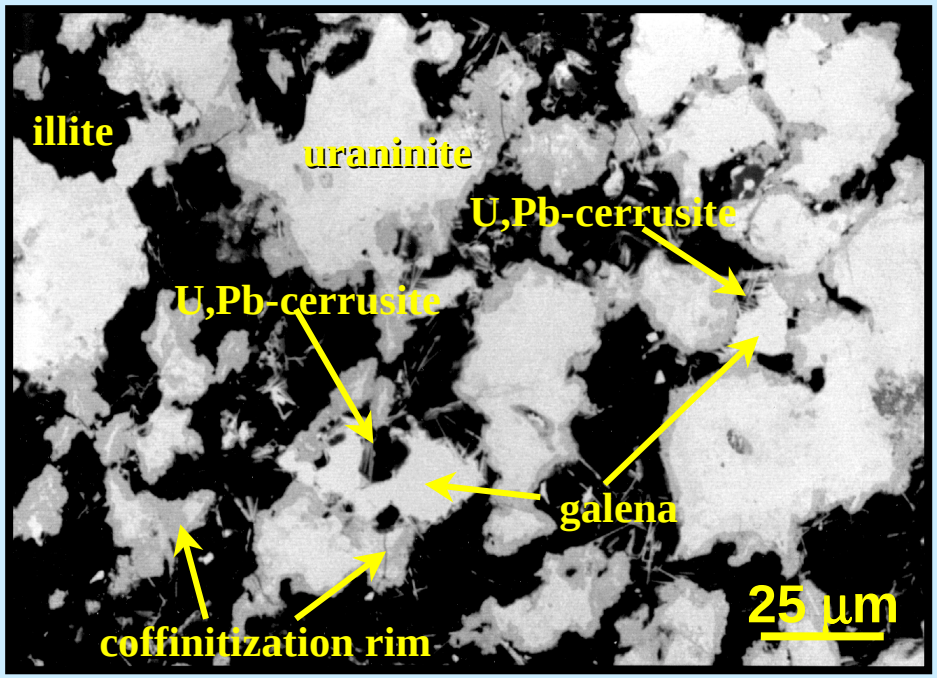

Fig. 4.2: Uraninite in the core of the Ok□obondoreactor. The uraninite is partially coffinitized that is rarely observed in the core of this reactor.

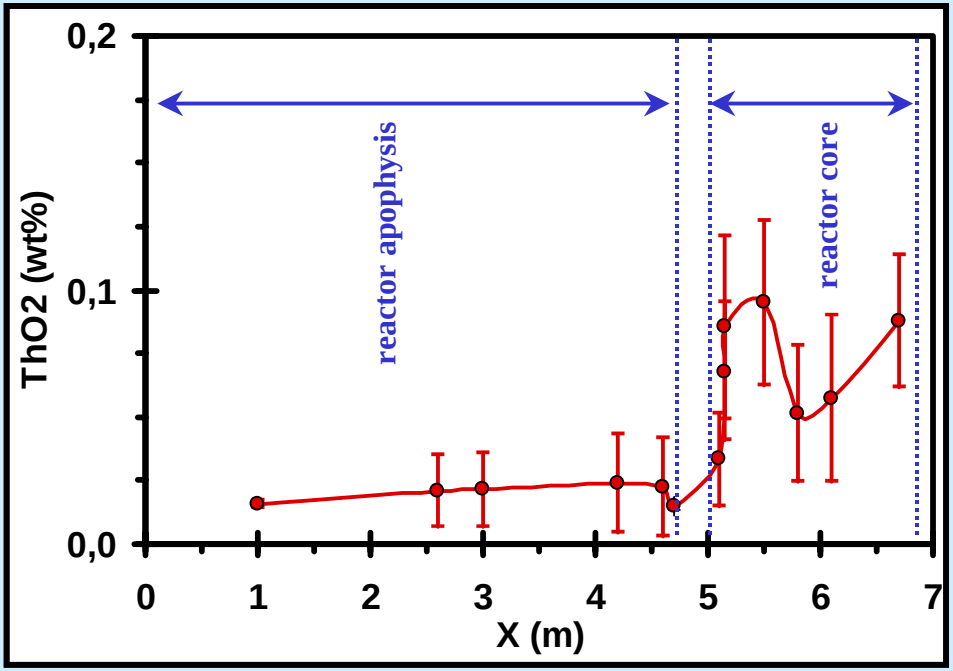

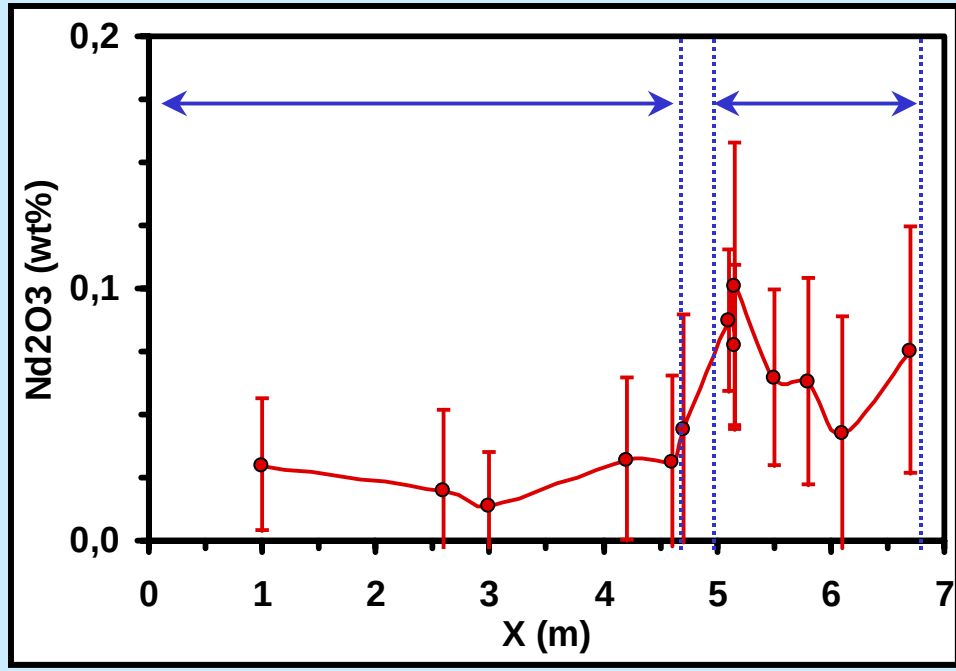

Fig. 4.3: Chemical variation of fissiogenic trace elements in uraninite along the Ok□obondo reactor zone. The data were collected from specimen 131, 127, 118, 117, 116, 9, 5, 84a, 84b, 12, 83, 113, and 82 (see Fig. 4.1). Similar variations were also observed for Zr (^{90}Sr) and Ce.

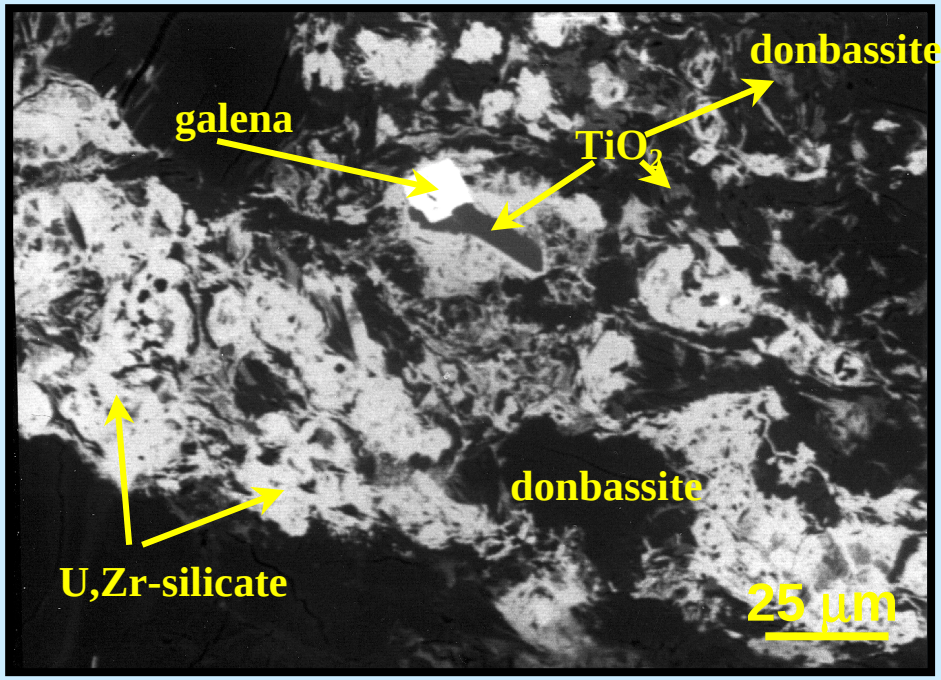

Fig. 4.4: U-Zr-silicate in fracture veinlets of the hydrothermal alteration halo above the Ok□obondoreactor core.

Table 4.2: Composition of the most Zr-rich U-Zr-silicate analyses that were found in specimen number 8.

UO_2	51.26	46.56	40.54
ThO_2	0.17	0.12	0.17
SiO_2	13.48	16.53	16.19
TiO_2	1.65	0.73	0.56
ZrO_2	18.29	21.32	24.29
PbO	0.00	0.04	0.02
FeO	0.14	0.16	0.12
CaO	2.66	2.66	2.86
Al_2O_3	0.95	1.32	1.40
P_2O_5	1.48	1.33	1.18
SO_3	0.00	0.03	0.04
Ce_2O_3	0.60	0.59	0.62
Nd_2O_3	0.31	0.43	0.42
Total	90.99	91.81	88.42

Phases with Metallic Fission Products

Ruthenium (including the daughter of ^{99}Tc) was present in accessory Ru-S-arsenides that occur as µm sized grains at uraninite grain-boundaries in the reactor (Fig. 4.5). The release of Ru (and Tc) may have occurred during syn-criticality diffusion and uraninite corrosion, but could also have occurred contemporaneous with a thermally-induced lead-loss 1000 - 750 Ma ago.

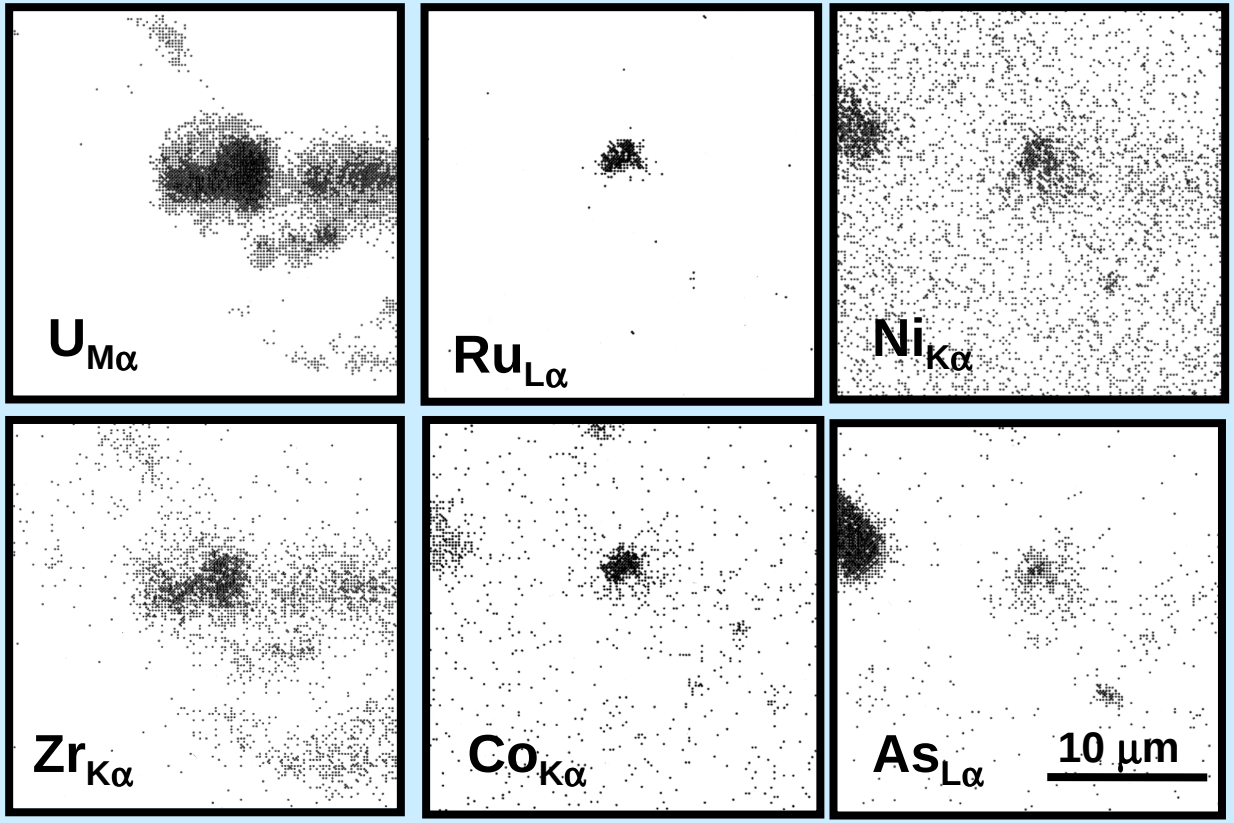

Fig. 4.5: X-ray maps of a Ru-S-arsenide grain associated with U-Zr-silicate immediately below the core of the Ok□obondonatural fission reactor.

Conclusions

The results show evidence for long-term retardation of nuclear reaction products in the geosphere by uraninite and accessory phases under reducing conditions. Long-term stability of uraninite is also indicated despite lead-loss and chemical alteration 1000 - 750 Ma ago.

5. A Zr- AND Si-RICH URANIUM PHASE FROM CENTRAL CITY DISTRICT, COLORADO

Uraninite coexisting with a Zr- and Si-rich uranium phase was observed in a Tertiary (40 to 2 Ma) arkosic sandstone from the Central City District, Gilpin County, Colorado. Back scattered electron (BSE) images and energy dispersive spectrum (EDS) analysis showed that the Zr- and Si-rich uranium phase occurred as inclusions or altered domains within the uraninite (Fig. 5.1).

Mineral Chemistry

Results from electron microprobe analyses showed systematic increases in SiO_2, ZrO_2, FeO, and P_2O_5 components as function of decreasing UO_2 (Fig. 5.2). There is a positive correlation between ZrO_2 and SiO_2, suggesting that the coexisting phase contains a U-Zr-silicate component, e.g., coffinite. The Zr- and Si- rich uranium phase may have formed contemporaneously with uraninite or formed during partial alteration of uraninite causing increased concentrations of Zr, Si, Fe and P.

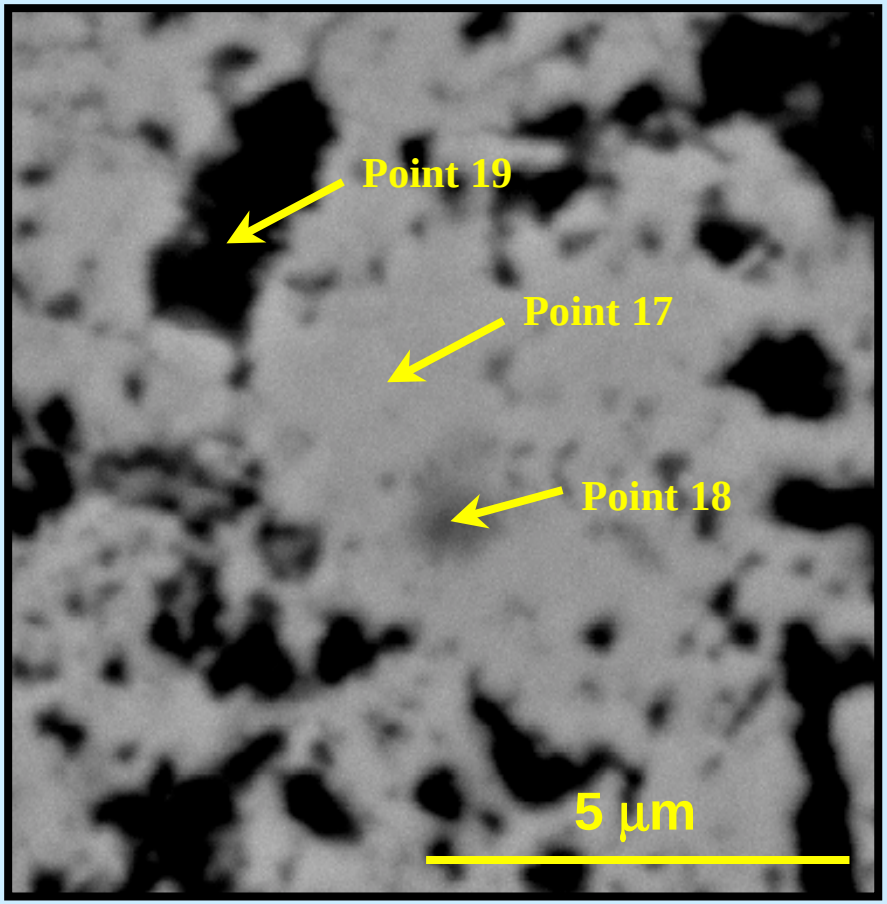

Table 5.1: Compositional comparison of normal uraninite and Zr-Si-rich uranium phase.

Oxide (wt.%)	normal uraninite	Zr-Si-rich U-phase
UO_2	90.2-96.5	78.3-90.4
ZrO_2	1.1-1.7	2.6-8.3
SiO_2	0.3-0.6	1.0-8.3

Fig. 5.1: Textural relation between "normal" uraninite and Zr-Si-rich uranium phase in sandstone from the Central City District. The numbers (17, 18, and 19) refer to the EDS spectra shown below.

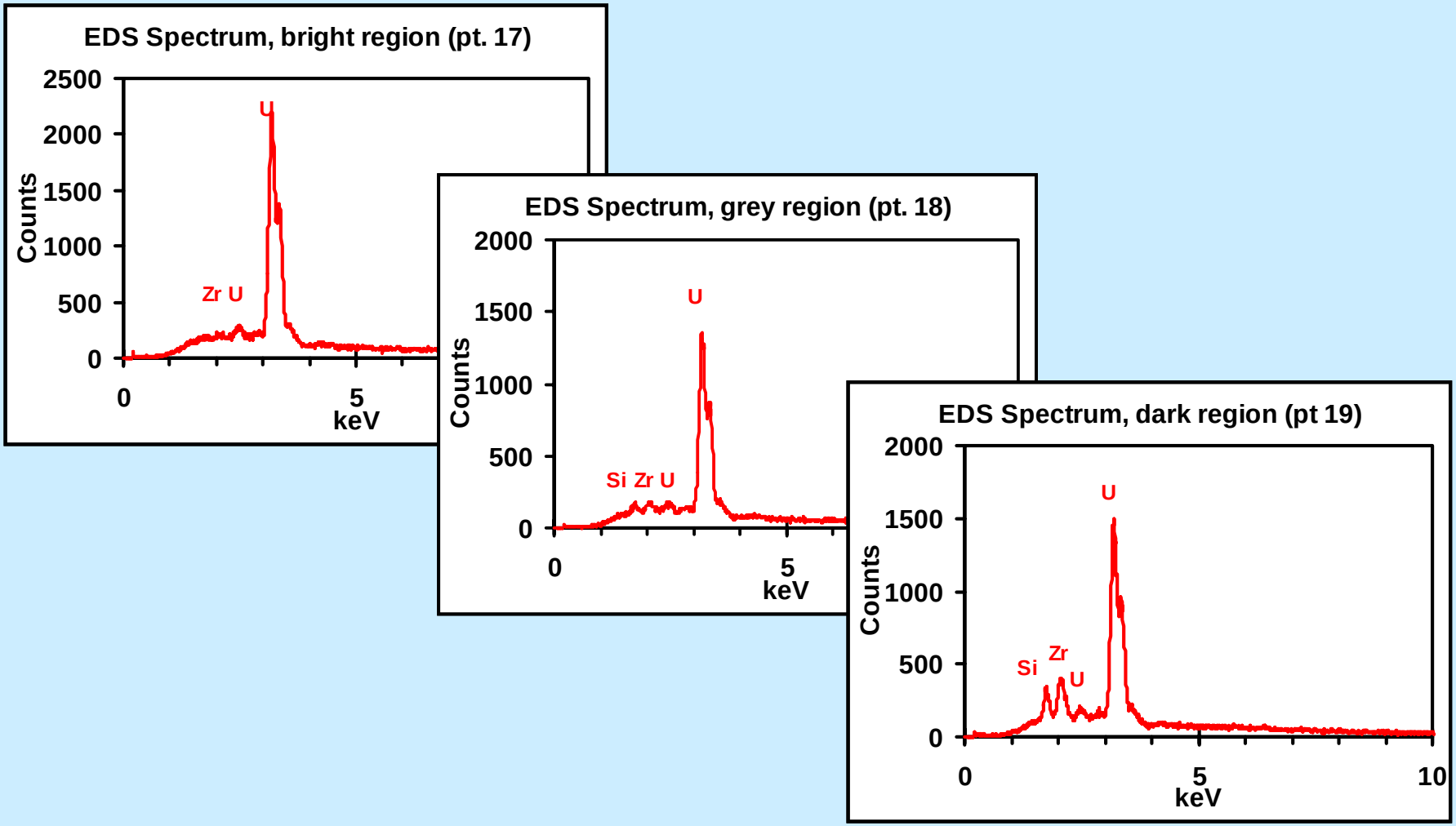

Fig. 5.2: EDS spectra of points 17, 18, and 19 in Fig. 5.1, illustrating increases in Zr and Si in the dark regions of the BSE image

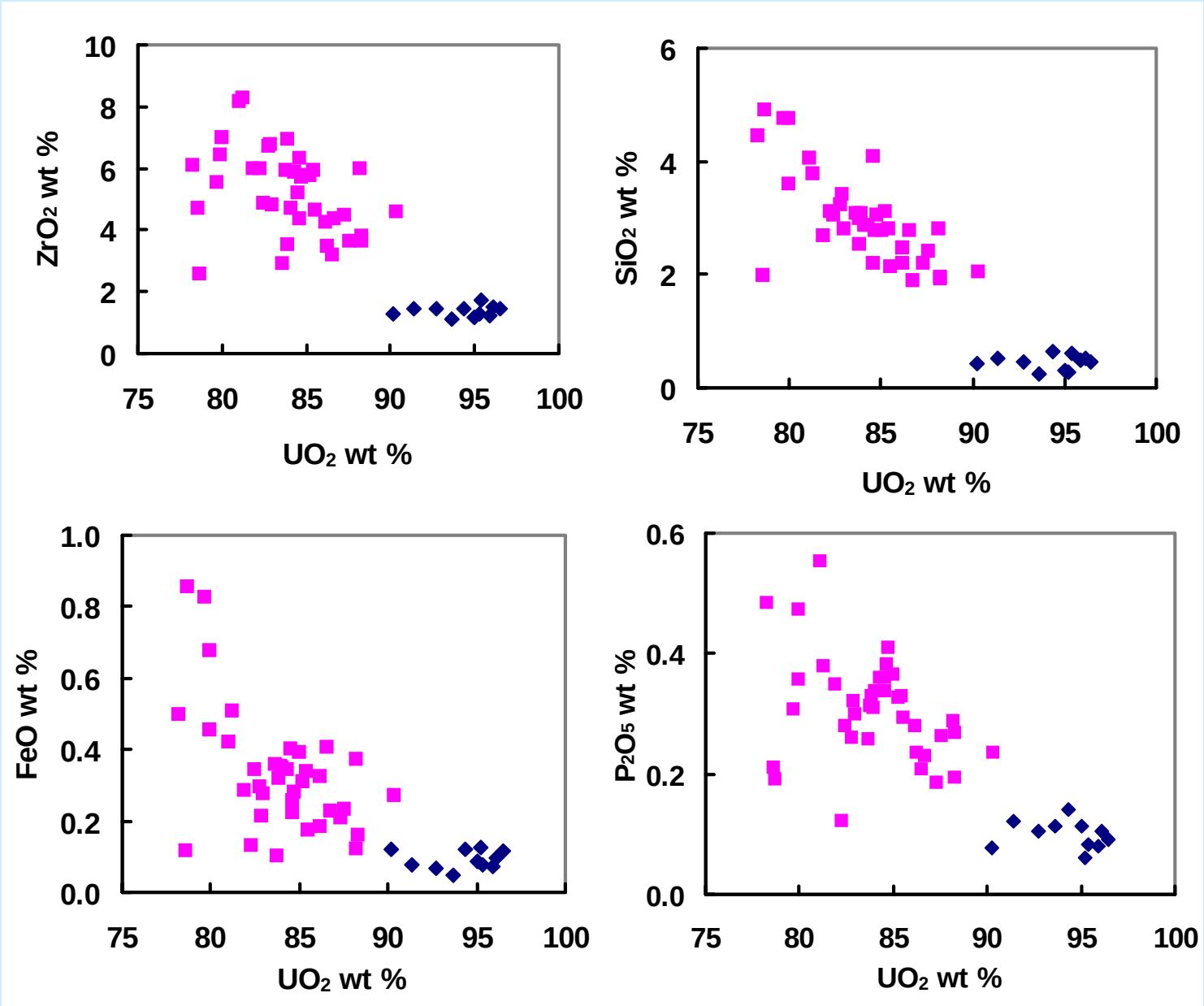

Fig. 5.3: Scatter diagrams showing the variation in a) ZrO_2, b) SiO_2, c) FeO, and d) P_2O_5 as function of UO_2. Square: Zr-Si-rich phase; diamond: uraninite

Conclusions

Textural relationships suggest that the uraninite may have been partially altered. Zr and Si were incorporated into the resultant uranium phase that contains lower UO_2 and higher ZrO_2, SiO_2 , FeO and P_2O_5; other trace elements are low or below EMPA detection limits. Enrichment of Si in uraninite indicates coffinitization; pyritization suggests a reducing condition. The increase of Si and P in the uranium phase suggests the existence of uranium silicate or phosphate components, which generally have higher a capability to incorporate fission products and radionuclides

RESULTS

The main results are divided into two general sections: studies of uraninite corrosion and long-term behavior under oxidizing and reducing conditions, respectively:

Oxidizing conditions: The study of uraninite alteration behavior under oxidizing conditions includes theoretical work on thermodynamic parameter estimates for important U^{6+} phases, retardation of Se and Tc in U^{6+} phases, and trace element retardation in natural uraninite corrosion products in specimens from the Colorado Plateau.

Reducing conditions: Analysis of uraninite and the behavior of nuclear reaction products under reducing conditions include studies of the Okélobondo natural fission reactor in Gabon and chemical characterization of a Zr and Si rich U-phase coexisting/replacing uraninite from the Colorado Plateau.

APPLICATIONS

- **The model for estimating the thermodynamic formation energies and enthalpies of formation is an important tool for performance assessment calculations used in predicting the phase assemblages that will form during corrosion of SNF.**

- **Theoretical evaluations of the Se and Tc behavior during oxidative corrosion of SNF shows that Se can be retarded. Tc remains a problem for the successful long-term performance of a SNF waste repository under oxidizing conditions.**

- **Preferred retardation of trace elements (e.g., REE) in uranyl phases during natural corrosion of uraninite supports theoretical studies that have indicated a retention capacity of several transuranium (TRU) elements in uranyl phases that form during corrosion of SNF.**

- **Retardation of U, (Pu), Th, (Sr), Zr, Ru, (Tc), and REE in uraninite and accessory phases that formed during syncriticality corrosion of uraninite in the 2 Ga old Oklo natural fission reactors shows that long-term mineralogical fixation of nuclear reaction products is possible under reducing conditions.**

- **Natural alteration of uraninite under reducing conditions can lead to the formation of U-Zr-silicate and suggests long-term retention capacity of fissiogenic Zr in secondary U-silicate.**

ACKNOWLEDGEMENTS

The research team gratefully acknowledge the financial support from the Environmental Management Science Program under the US Department of Energy (Contract # DE-FG07-97ER 14816). In the research on the Okélobondo natural fission reactor we are also grateful to be funded by the Swedish Nuclear Waste Management Company (SKB) through the EU-research program Oklo-Natural Analogue - Phase II.

The work completed in the Environmental Science Management Program was also based on collaboration and publication with scientists from a number of other institutions:

- ***Dr. Peter Burns*, Notre Dame University.**
- ***Dr. Jordi Bruno*, QuantiSci, Barcelona, Spain.**
- ***Dr. Ignasi Casas*, Department of Chemistry, UPC, Barcelona, Spain**
- ***Dr. Fanrong Chen*, Guangzhou Institute of Geochemistry, Chinese Academy of Sciences, Wushan, P.R. China.**
- ***Professor Sue Clark*, Department of Chemistry, Washington State University**
- ***Dr. Mostafa Fayek*, Center of Isotope Geochemistry, Oak Ridge National Laboratory.**
- ***Dr. Francois Gauthier-Lafaye*, Centre National de la Recherche Scientifique, Strasbourg, France**
- ***Dr. Sidsel Grundvig*, University of Aarhus, Denmark.**
- ***Professor Frank Hawthorne*, Department of Geological Sciences, University of Manitoba, Canada.**
- ***Professor Janusz Janeczek*, Faculty of Earth Sciences, University of Silesia, Poland.**
- ***Professor Takashi Murakami*, Mineralogical Institute, Tokyo University, Japan**
- ***Dr. Juan de Pablo*, Department of Chemical Engineering, UPC, Barcelona, Spain.**

SELECTED PUBLICATIONS

- *Chen F., Ewing R.C., and Clark S.B. (1999) The Gibbs free energies and enthalpies of formation of uranium (VI) phases: An empirical method of prediction. American Mineralogist, 84(4), 650-654.*
- *Chen F., Burns P.C., and Ewing R.C. (1999) ^{79}Se: Geochemical and crystallo-chemical retardation mechanisms. Journal of Nuclear Materials 275, 81-94.*
- *Chen F., Burns P.C., and Ewing R.C. (2000) Near-field behavior of ^{99}Tc during the oxidative alteration of spent nuclear fuel. Journal of Nuclear Materials 278, 225-232.*
- *Jensen K.A. and Ewing R.C. (2000) The Okelobondo natural fission reactor, southeast Gabon: geology, mineralogy and retardation of nuclear reaction products. Geological Society of America Bulletin (accepted).*
- *Zhao D. and Ewing R.C. (2000) Alteration Products of Uraninite from the Colorado Plateau. Radiochimica Acta (accepted).*
- *Zhao D. and Ewing R.C. (1999) Zirconium-rich uraninite from the Central City District, Gilpin County, Colorado. Geological Society of America Annual Meeting Abstract and Program, 1999, p. A-135.*

FURTHER INFORMATION

- *Mailing address: Dept. of Nuclear Engineering & Radiological Sciences, The University of Michigan, 2355 Bonisteel Blvd., Ann Arbor, MI 48109*
- *Phone: (734) 647-8529*
- *Fax: (734) 647-8531*
- *E-Mail: rodewing@umich.edu*
- *Web site: http://relw.engin.umich.edu/*